SINGLE-PARTICLE INCLUSIVE DISTRIBUTION AT LARGE p_T IN PARTON MODELS

By W. Furmański and J. Wosiek

Institute of Physics, Jagellonian University, Cracow*

(Received March 10, 1977)

The predictions of parton models for the single-particle distribution in the large p_T region are analysed. An explicit expression for the slope B in the formula $E\frac{d\sigma}{d^3p} = \frac{c}{p_T^N} e^{-Bx_T}$ is derived. It is shown that the weak rapidity dependence of B, observed at ISR implies the hard scattering cross-section $\frac{d\sigma}{dt}$ to be approximately independent of energy *at fixed* p_T.

1. Introduction

In this paper we study the single-particle distribution of large p_T mesons produced in high-energy collisions. Taking the parton model as our basic assumption we attempt to determine what the available data imply for the interaction of elementary hadronic constituents at small distances. Our main result is that, in order to describe properly the rapidity dependence of the large p_T spectrum it is necessary that the elementary hard scattering cross-section $\frac{d\sigma}{dt}$ depends approximately only on p_T.

In parton model the fast moving hadron is treated as a collection of non-interacting point-like constituents — partons. In hadron-hadron collision these two parton clouds go through each other and the large p_T particles are produced as a result of the wide angle elastic scattering of fast constituents.

There is a number of parton models which have been proposed to describe the large p_T phenomena (see, e. g. Ellis talk at London Conference 1975). They differ in the type of constituents which are assumed to give the leading contribution to the wide angle scattering and in the shape of the hard scattering cross-section.

* Address: Instytut Fizyki UJ, Reymonta 4, 30-059 Kraków, Poland.

However, in spite of these differences in details all these models predict:

a) power-like fall off of the single-particle inclusive yields in the transverse momentum p_T,

b) large p_T scaling, i. e. the dependence on energy only by the scaling variable $x_T = \frac{2p_T}{\sqrt{s}}$,

c) coplanarity and the jet structure in the large p_T events.

These predictions are confirmed by the recent experiments [1–4] so that it is likely that the parton model can provide a proper dynamical description of large p_T production.

In this situation it seems worthwhile to go one step further and ask whether the data can tell us something more about the details of the model; in particular, about the type of constituents which undergo the hard scattering and the angular dependence of the hard scattering itself. Such information should be very valuable (in fact, necessary) for finding the correct interactions of hadronic constituents at small distances.

The purpose of this paper is to attempt such an analysis. We derive the (approximate) analytic formula for the single-particle distributions, starting from the simple parametrization of the quark model input. We then compare the results with the data from CERN-ISR experiments. As shown below the data restrict quite severily the angular dependence of hard scattering as well as the type of constituents dominating in meson production at large p_T.

We start with a brief review of the present experimental status in the large p_T production on the single-particle level in the ISR region ($x_T < 0.3$, $|y| < 1$):

1) p_T dependence: the single-particle spectrum falls off approximately like some power of p_T, for p_T 2 GeV/c with a power $N \approx 8$ for mesons and $N \approx 12$ for barions [1, 2, 4];

2) s dependence: large p_T scaling is satisfied to a good approximation, i. e. the single-particle distribution depends on s only by the scaling variable $x_T = \frac{2p_T}{\sqrt{s}}$ [1, 2, 4]:

$$E \frac{d\sigma}{d^3p} \approx \frac{c}{p_T^N} g(x_T, y). \tag{1.1}$$

For $y = 0$ fits of type

$$E \frac{d\sigma}{d^3p} \approx \frac{c}{p_T^N} e^{-Bx_T} \tag{1.2}$$

with $B \approx 13$ for π^0 and $B \approx 15$ for π^+, π^- seem to describe the data rather well for $x_T < 0.3$ [1, 2, 4];

3) y dependence: for small y ($|y| < 1$) the function $g(x_T, y)$ depends weakly on y. One can see it in Fig. 1a, where $g(x_T, y)$ is presented for $y = 0.0$ and $y = 0.75$. The slope B in (1.2) seems to be only slightly greater at $y = 0.75$.

The relevance of the scaling variable $x_E = x_T \cosh(y)$ assumed by some authors as the typical one for the parton models (what is not true it general, as we show in the next Section) is tested in Fig. 1b (Figs 1a and 1b are taken from Ref. [2]). One can see there

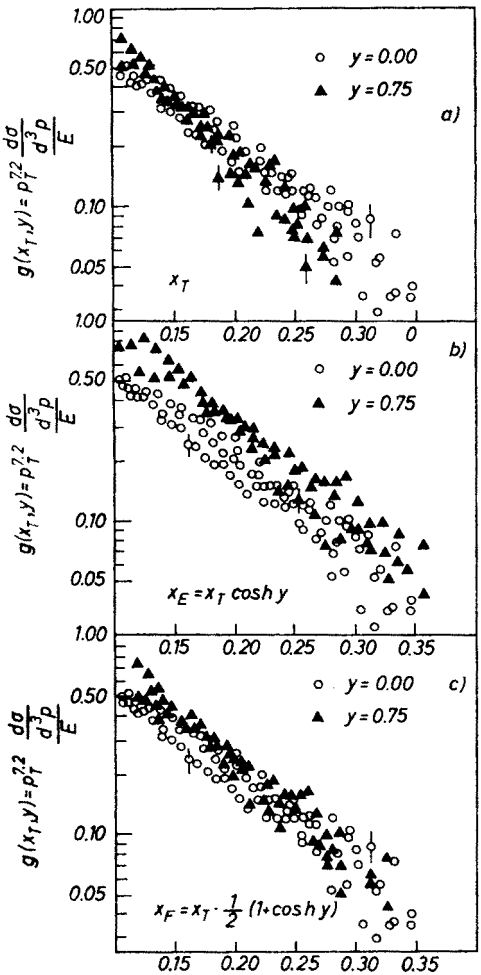

Fig. 1. The scaling function $g(x_T, y)$ (Ref. [2]): a) $g(x_T, y)$ versus x_T: test for scaling $g(x_T, y) = \tilde{g}(x_T)$, b) $g(x_T, y)$ versus $x_E = x_T \cosh y$: test for scaling $g(x_T, y) = \tilde{g}(x_E)$, c) $g(x_T, y)$ versus $x_F = \frac{1}{2} x_T(1+\cosh y)$: test for scaling $g(x_T, y) = \tilde{g}(x_F)$

that the data does not favour the scaling of type $g(x_T, y) = \tilde{g}(x_E)$. Thus the rapidity dependence can be summarized by the formula

$$E \frac{d\sigma}{d^3p} = \frac{c}{p_T^N} e^{-B(y)x_T}, \tag{1.3}$$

where $B(y)$ depends very weakly on y. In particular, $B(y) = B(0)\cosh(y)$ gives much too strong rapidity dependence than observed experimentally.

For reasons which will be clear in the next Section we have tried to test scaling of type

$$g(x_T, y) = \tilde{g}(\tfrac{1}{2} x_T(1+\cosh y)),$$

or $B(y) = B(0)\,\frac{1}{2}\,(1+\cosh y)$. As seen from Fig. 1c, it fits the data rather well, especially for larger values of x_T.

To observe the y dependence of B we have fitted the formula (1.3) (or, in another words, (1.2) for $y = 0$ and $y = 0.75$ separately) to the ACHM data (Ref. [2]); the result is presented in Fig. 2. Solid lines correspond to $B(y)$ functions considered above. Hence we

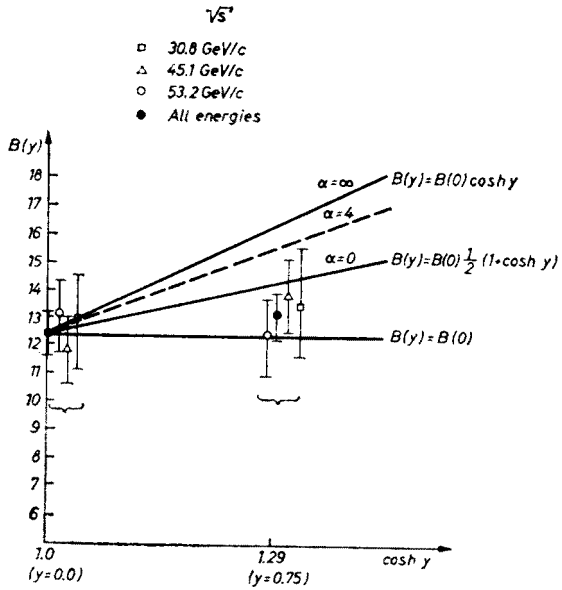

Fig. 2. y dependence of the slope B in the formula (1.3). Points are results of the fit to the ACHM data (Ref. [2]). Solid lines correspond to the functions $B(y)$ tested in Fig. 1. Dashed line is the prediction of the model with isotropic (at fixed s) hard scattering for $\langle x_T \rangle = 0.2$

conclude once more that $B(y) = B(0)\cos y$ is excluded by the data. As seen from Fig. 2, the value of B for $y = 0.75$ lies between $B(y) = B(0)$ and $B(y) = B(0)\,\frac{1}{2}\,(1+\cosh y)$.

In the present paper we find an explicit (although approximate) expression for $g(x_T, y)$ valid in the ISR region for most versions of the parton models. It has the form suggested by (1.3), where

$$B(y) = B(0)\,[\beta_1 \cosh y + \beta_2\,\tfrac{1}{2}\,(1+\cosh y)], \qquad \beta_1+\beta_2 = 1. \tag{1.4}$$

$B(0)$ is determined by the structure functions involved in a model, β_1 and β_2 are sensitive to the angular dependence of the hard scattering.

In particular, if the hard scattering cross section does not depend on angle (energy) *at fixed* p_T, i. e.

$$\frac{d\sigma}{dt}(p_T, \theta) = \frac{d\sigma}{dt}(p_T, 90^\circ), \tag{1.5}$$

then $\beta_1 = 0$, $\beta_2 = 1$, while if it does not depend on angle *at fixed* s, i. e.

$$\frac{d\sigma}{dt}(s, \theta) = \frac{d\sigma}{dt}(s, 90^\circ) \tag{1.6}$$

then $\beta_1 = 1$, $\beta_2 = 0$.

Comparison of the formula (1.4) with properties 2) and 3) of the experimental yield imply the following constraints on parton models:

a) $B(0) = 13$–15 for π production,

b) $\beta_1 \ll \beta_2$.

Thus our conclusion is that to reproduce weak rapidity dependence of the single-particle distribution one has to build the model with the hard scattering which does not depend on energy at fixed p_T (Eq. (1.5)).

On the contrary to it, models with isotropic (at fixed s) hard scattering (Eq. (1.6)) are far from beeing able to reproduce b), i. e. they give too sharp rapidity dependence and seem to be excluded by our analysis.

Values of $B(0)$ are calculated for π production in the Constituent Interchange Model (CIM) [5]. We find a) to be approximately satisfied by all leading subprocesses with the double-jet fragmentation in the final state, while the quasi-exclusive contributions give too small value of $B(0)$.

2. *Calculation of the single-particle distribution*

Let us start with the general formula for the single-particle distribution in the parton models (see Fig. 3 for notation):

$$\left(\frac{\frac{d\sigma}{d^3p_1}}{E_1}\right)_{AB\to 1+X} = \int dx_{c_1} \int dx_{c_2} G_{c_1|A}(x_{c_1}) G_{c_2|B}(x_{c_2}) \left(\frac{\frac{d\sigma}{d^3p_1}}{E_1}\right)_{c_1c_2\to 1+X} + (A \leftrightarrow B), \tag{2.1}$$

where $G_{c_1|A}(x_{c_1})$, $G_{c_2|B}(x_{c_2})$ are the structure functions of constituents c_1, c_2 in incoming protons A, B, respectively, for which we take the standard form

$$G_{c_1|A}(x_{c_1}) = \frac{n_{c_1|A}}{x_{c_1}}(1-x_{c_1})^{g_{c_1|A}}, \qquad G_{c_2|B}(x_{c_2}) = \frac{n_{c_2|B}}{x_{c_2}}(1-x_{c_2})^{g_{c_2|B}} \tag{2.2}$$

(transverse motion of c_1 and c_2 is neglected). Powers $g_{c_1|A}$, $g_{c_2|B}$ are determined by the formula

$$g_{c|A} = 2m_{c|A} - 1,$$

where $m_{c|A}$ is the minimal number of quarks which must be slowed down in A to produce c with $x \approx 1$ (e. g. $g_{q|P} = 3$, $g_{q|\pi} = 1$, $g_{\pi|P} = 5$ etc.). Inclusive distribution for the subprocess $c_1c_2 \to 1+X$ can be written as

$$\left(\frac{\frac{d\sigma}{d^3p_1}}{E_1}\right)_{c_1c_2\to 1+X} = \int \frac{d^3p_{J_1}}{E_{J_1}} \left(\frac{\frac{d\sigma}{d^3p_{J_1}}}{E_{J_1}}\right)_{c_1c_2\to J_1J_2} \left(\frac{\frac{dN}{d^3p_1}}{E_1}\right)_{J_1\to 1+X} + (J_1 \leftrightarrow J_2). \tag{2.3}$$

Since the hard scattering is assumed to be the elastic one

$$\left(\frac{d\sigma}{\frac{d^3p_{J_1}}{E_{J_1}}}\right)_{c_1c_2\to J_1J_2} = \frac{\hat{s}}{\pi}\delta(\hat{s}+\hat{t}+\hat{u})\left(\frac{d\sigma_H}{d\hat{t}}\right)_{c_1c_2\to J_1J_2} \tag{2.4}$$

(quantities with $\wedge$ refer to c_1c_2 CM frame, without $\wedge$ to AB CM frame; see Fig. 3).

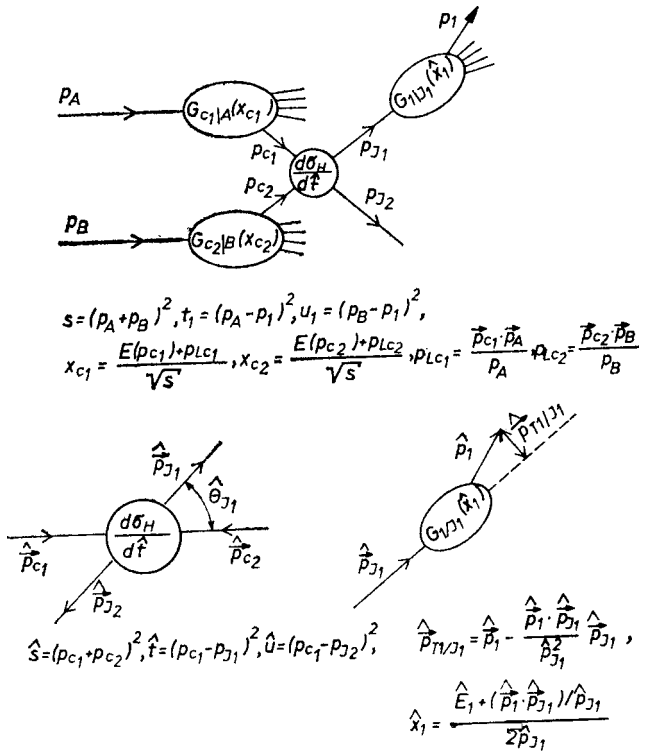

Fig. 3. Definition of the variables used in text

From the dimensional analysis (Brodsky-Farrar counting rules [6]) which is assumed to work in the wide angle region $s\to\infty$, $t\to\infty$, t/s fixed

$$\left(\frac{d\sigma_H}{d\hat{t}}\right)_{c_1c_2\to J_1J_2} = \frac{c_0}{\hat{s}^n} f\left(\frac{\hat{t}}{\hat{s}}\right), \tag{2.5}$$

where $n = N_q - 2$, N_q beeing the number of external quark legs in the hard scattering amplitude.

The simplest formula for the jet J_1 fragmentation (zero width approximation) reads

$$\left(\frac{dN}{\frac{d^3p_1}{E_1}}\right)_{J_1\to p_1+X} = \frac{1}{\pi}\delta(\hat{p}^2_{T_1|J_1})\hat{x}_1 G_{1|J_1}(\hat{x}_1), \tag{2.6}$$

where $\hat{p}_{T1|J_1}$ is the transverse component of $\hat{\vec{p}}_1$ relative to the jet axis $\hat{\vec{p}}_{J_1 1}$ and $\hat{x}_1 = \dfrac{\hat{E}_1 + \hat{p}_{T1}}{2\hat{p}_{J_1}} \approx \dfrac{p_{T1}}{p_{TJ_1}}$.

The calculation of the integrals involved in (2.1) and (2.3) is presented in the Appendix, here we wish only to describe briefly the method. It can be proved (see Appendix) that the symmetrization $A \leftrightarrow B$ can be reduced approximately to the replacement

$$f\left(\frac{\hat{t}}{\hat{s}}\right) \to f_{sym}\left(\frac{\hat{t}}{\hat{s}}, \frac{\hat{u}}{\hat{s}}\right) = f\left(\frac{\hat{t}}{\hat{s}}\right) + f\left(\frac{\hat{u}}{\hat{s}}\right)$$

in (2.5). Now, using the well-known properties of the symmetric functions and the two-body condition $\hat{s} + \hat{t} + \hat{u} \approx 0$ we find that f_{sym} depends only on the one variable

$$\lambda = \frac{\hat{s}^2}{4\hat{t}\hat{u}} = \frac{1}{\sin^2 \hat{\theta}_{J_1}} = \cosh^2 \hat{y}_{J_1}$$

since

$$f_{sym}\left(\frac{\hat{t}}{\hat{s}}, \frac{\hat{u}}{\hat{s}}\right) = \hat{f}\left(\frac{\hat{t}}{\hat{s}} \frac{\hat{u}}{s}, \frac{\hat{t}}{\hat{s}} + \frac{\hat{u}}{\hat{s}}\right) \equiv h(\lambda). \tag{2.7}$$

Thus the symmetrized hard scattering cross-section can be written as follows:

$$\left(\frac{d\sigma_H}{d\hat{t}}\right)_{sym} = \frac{c_0}{\hat{s}^n} f_{sym} = \frac{c_0}{\hat{s}^n} h(\lambda) = \frac{c_0}{(4p_{TJ_1}^2)^n} H(\lambda), \tag{2.8}$$

where

$$H(\lambda) \equiv \frac{1}{\lambda^n} h(\lambda). \tag{2.9}$$

Note that the conditions (1.5) and (1.6), considered in the Introduction can be simply expressed in terms of H and h functions

$$\frac{d\sigma_H}{d\hat{t}}(p_T, \theta) = \frac{d\sigma_H}{d\hat{t}}(p_T, 90°) \Leftrightarrow H(\lambda) = \text{const}, \tag{2.10}$$

$$\frac{d\sigma_H}{d\hat{t}}(s, \theta) = \frac{d\sigma_H}{dt}(s, 90°) \Leftrightarrow h(\lambda) = \text{const}. \tag{2.11}$$

In general, the function $H(\lambda)$ is determined by the angular dependence of the hard scattering cross-section and thus it depends on the details of a particular model. However, since $H(\lambda)$ decreases for large λ due to the factor $1/\lambda^n$ (or at least remains constant) in almost all proposed hard scattering models, we can use for the integration purposes the approximate form

$$H(\lambda) = H(\cosh^2 \hat{y}_{J_1}) \approx H(1) e^{-\alpha \hat{y}_{J_1}^2}. \tag{2.12}$$

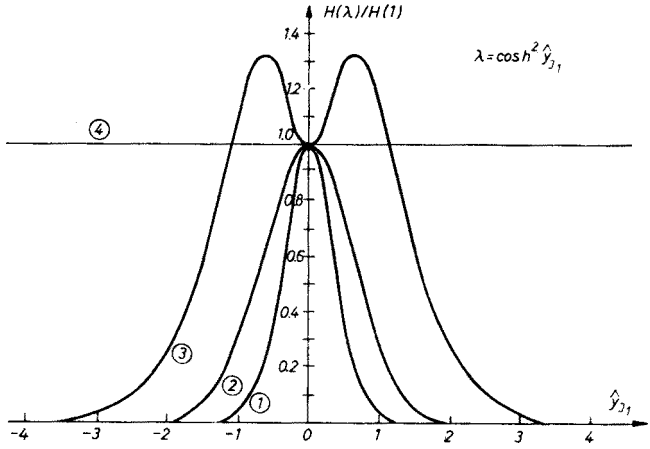

Fig. 4. Function $H(\lambda)/H(1)$ for some hard scattering models. Numbers coincide with those from Table I

The detailed shape of $H(\lambda)$ and the values of α (numerical fits) for some parton models can be found in Fig. 4 and in Table I, respectively. If $H(\lambda)$ decreases with λ for $\lambda \geqslant 1$ then one can use for by-hand estimates the steepest descent formula for α

$$\alpha \approx n - \frac{h'(\lambda)}{h(\lambda)}\bigg|_{\lambda=1}. \tag{2.13}$$

In particular, we find from the above that $\alpha = 0$ for the angular dependence given by (2.10) and $\alpha = n$ (= 4 for meson production) for the one given by (2.11).

TABLE I

The function $H(\lambda)/H(1)$ and the value of α for some hard scattering models. Values of α are the results of fit $H(\lambda) = H_1 e^{-\alpha \hat{y}_{J_1}^2}$

No	Model	$\frac{d\sigma_H}{d\hat{t}}$	$H(\lambda)/H(1)$	α
1	isotropic hard scattering (at fixed s)	$\frac{c_0}{\hat{s}^4}$	$\frac{1}{\lambda^4}$	3.77
2	CIM (spin 0 quarks) $\pi^+p \to \pi^+p$	$\frac{c_0}{\hat{s}^4}\left(\frac{\hat{s}}{-\hat{u}}\right)^2$	$\frac{2}{\lambda^2} - \frac{1}{\lambda^3}$	1.26
3	CIM (spin 1/2 quarks) $\pi^+p \to \pi^+p$	$\frac{c_0}{\hat{s}^4}\left(\frac{\hat{s}}{-\hat{u}}\right)^3$	$\frac{4}{\lambda} - \frac{3}{\lambda^2}$	0.33
4	isotropic hard scattering (at fixed p_T)	$\frac{c_0}{\hat{s}^4}\left(\frac{\hat{s}}{\hat{t}} + \frac{\hat{s}}{\hat{u}}\right)^4$	1	0.0

With $H(\lambda)$ given by (2.12) the integrals in (2.3) can be easily performed by means of the saddle point method (see Appendix for details) and the final result reads

$$\left(\frac{d\sigma}{\frac{d^3p_1}{E_1}}\right)_{AB\to 1+X} = \frac{c_{1|J_1}}{p_{T_1}^N} e^{-B(x_{T_1}y_1)x_{T_1}} + (J_1 \leftrightarrow J_2), \tag{2.14}$$

where $N = 2n$,

$$B(x_{T_1}, 0) = B(0, 0) \equiv B = \frac{1}{\langle \hat{x}_1 \rangle} (g_{c_1|A} + g_{c_2|B}),$$

$$\langle \hat{x}_1 \rangle = \frac{N-3}{N-2+g_{1|J_1}}, \tag{2.15}$$

$$B(x_{T_1}, y_1) = B\left[\frac{Bx_{T_1}}{Bx_{T_1}+\alpha} \tfrac{1}{2}(1+\cosh y_1) + \frac{\alpha}{Bx_{T_1}+\alpha} \cosh y_1\right], \tag{2.16}$$

$$c_{1|J_1} = \langle x_1^{N-2} \rangle_{J_1} c_{J_1}, \tag{2.17}$$

$$c_{J_1} = \frac{2}{\pi} \frac{c_0}{4^N} n_{c_1|A} n_{c_2|B} H(1) \sqrt{\frac{\pi}{Bx_{T1}+\alpha}}, \tag{2.18}$$

$$\langle \hat{x}_1^{N-2} \rangle_{J_1} = \int_0^1 d\hat{x}_1 \hat{x}_1^{N-2} G_{1|J_1}(\hat{x}_1) = n_{1|J_1} \frac{(g_{1|J_1})!(N-3)!}{(N-2+g_{1|J_1})!}. \tag{2.19}$$

For the quasi-exclusive limit ($1 = J_1$) one has to take $\langle \hat{x}_1 \rangle = \langle \hat{x}_1^{N-2} \rangle_{J_1} = 1$.

3. Discussion and conclusions

Formula (2.14) gives the prediction for the single-particle distribution in the large p_T ($p_T > 2$ GeV/c), small x_T ($x_T < 0.3$), small y ($|y| < 1$) region, valid (approximately) for the broad class of the parton models. An interesting point is, that all the freedom due to the a priori undetermined angular dependence of the hard scattering cross-section appears to be reduced to one effective width parameter α. In the following we present the comparison of (2.14) with the experiment.

3.1. Value of B for $y_1 = 0$

As seen from (2.15) B is determined by the behaviour of the structure functions $G_{c_1|A}$, $G_{c_2|B}$, $G_{1|J_1}$ near $x = 1$ and by the power n in the hard scattering.

We present here the numerical results for π production in the CIM. Values of B for various CIM subprocesses are collected in Table II. For two-body resonant decay we take simply $G_{1|J_1}(\hat{x}_1) \sim \delta(\hat{x}_1 - \frac{1}{2})$. Comparison of the results from Table II with the data is presented in Fig. 5. Since parameters B and N in the formula (1.2) are strongly correlated,

TABLE II

Values of the slope B in the formula (2.14) for various subprocesses in the CIM

No	Subprocess	g_{1/J_1}	$g_{C_1/A}$	$g_{C_2/B}$	$\langle \hat{x}_1 \rangle$	B
1	$Mq \to Mq$	0	5	3	1	8.0
2	$Mq \to M(q \to M+X)$	1	5	3	5/7	11.2
3	$Mq \to (M \to M+X)q$	3	5	3	5/9	14.4
4	$Mq \to (M^* \to M+M')q$	—	5	3	1/2	16.0
5	$q\bar{q} \to M\bar{M}$	0	3	3	1	6.0
6	$q\bar{q} \to (M \to M+X)\bar{M}$	3	3	3	5/9	10.8
7	$q\bar{q} \to (M^* \to M+M')\bar{M}$	—	3	3	1/2	12.0
8	$M\bar{M} \to (q \to M+X)\bar{q}$	1	5	5	5/7	14.0

it is useful to work on the (B, N) plane, as proposed by the ACHM Collaboration, where the regions of the best fits to the ACHM and CCR data are presented. Dashed line gives the best value of B with fixed N for ACHM data. As seen from Fig. 5, there is some discrepancy between the ACHM and CCR data and therefore, if we fix $N = 8$ (which is indeed fixed for the leading subprocesses in Table II) then the allowed region for B extends

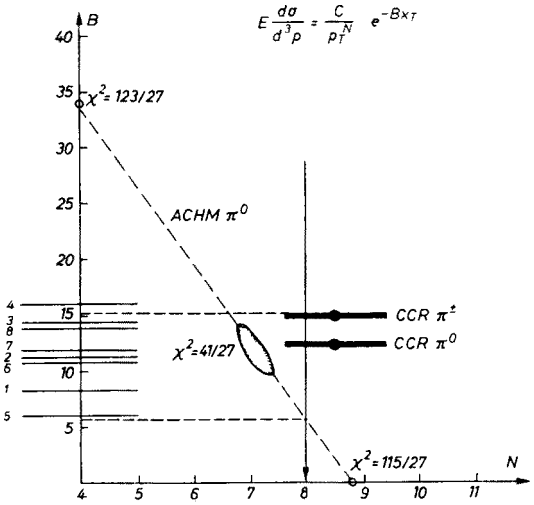

Fig. 5. CIM predictions for $B(0)$ on (B, N) plane. Numbers coincide with those from Table II

from 6 to 15. Almost all values of B from Table II fall into this region. Thus the present data are not able to discriminate in a definite manner between various subprocesses.

However, if one forgets for a moment about the discrepancy in N and compares results from Table II with the best fits for B to ACHM and CCR data (where the nice overlap is present), then the quasi-exclusive components seem to be excluded (see Fig. 6).

If further experiments give support to this guess, it can introduce very essential cut--offs among possible subprocesses in the CIM. The point is that if for some reason the quasi-exclusive limit of some subprocesses gives a negligible contribution (it would be desired to reproduce the experimental value of B), then all the inclusive versions of this subprocesses are even strongly supressed due to simple relation between the normalization constants (2.17). Since $n_{1|J_1}$ is typically of order of 1, $\langle x_1^{N-2}\rangle_{J_1}$ in (2.17) introduces the

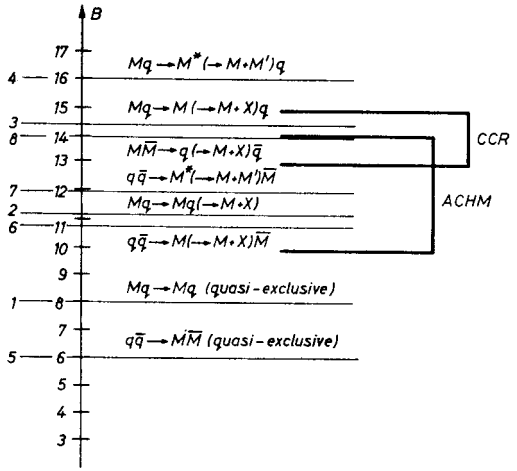

Fig. 6. Comparison of the CIM predictions for $B(0)$ with the region of the best fit for B to the ACHM and CCR data (Refs [2], [1])

suppresion by a factor $2.5 \cdot 10^{-2}$ for $g_{1|J_1} = 1$ and by a factor $2 \cdot 10^{-4}$ for $g_{1|J_1} = 3$. Thus, if one takes seriously this elimination, then, as seen from Fig. 6, the only subprocess which remains is the annihilation $M\overline{M} \to q\bar{q}$. However, more consistent experimental information is needed to decide if this guess can be turned into a definite statement.

3.2. Rapidity dependence of the single-particle distribution

The formula (2.16) can be written in the form given in the Introduction (Eq. (1.4))

$$B(x_{T1}, y_1) = B[\beta_1(x_{T1}) \cosh y_1 + \beta_2(x_{T1}) \tfrac{1}{2}(1+\cosh y_1)]$$

where

$$\beta_1(x_{T1}) = \frac{\alpha}{Bx_{T1}+\alpha}, \quad \beta_2(x_{T1}) = \frac{Bx_{T1}}{Bx_{T1}+\alpha}, \quad \beta_1(x_{T1})+\beta_2(x_{T1}) = 1.$$

Thus the rapidity dependence of the single-particle spectrum is determined by the relative values of β_1 and β_2, i. e. by Bx_{T1} and α. Two extreme cases $\beta_1 = 0$, $\beta_2 = 1$ ($\alpha = 0$) and $\beta_1 = 1$, $\beta_2 = 0$ ($\alpha = \infty$) were discussed in the Introduction (see Figs 1b, 1c, 2) and we have found there that for $\beta_1 = 0$, $\beta_2 = 1$ ($\alpha = 0$) a reasonable fit can be obtained, while $\beta_1 = 1$, $\beta_2 = 0$ ($\alpha = \infty$) gives too fast growth of B, i. e. too sharp rapidity dependence.

Thus the constraint for the hard scattering cross-section we find reads

$$\beta_1 \ll \beta_2 \Leftrightarrow \langle Bx_{T1} \rangle \gg \alpha \Leftrightarrow \frac{d\sigma_H}{d\hat{t}}(p_T, \theta) \approx \frac{d\sigma_H}{d\hat{t}}(p_T, 90°). \tag{3.1}$$

i. e. *the hard scattering should be independent of energy* (or, what is equivalent, of angle) *at fixed* p_T.

For the quantitative comparison of various models the parameter α can be used: the smaller value of α the weaker rapidity dependence of the single-particle spectrum predicted by a particular model. For the CIM with spinless quarks we have $\alpha \sim 1.3$. This is still comparable with $\langle Bx_{T1} \rangle$ (for $\langle x_{T1} \rangle = 0.2$ we have $\langle Bx_1 \rangle \approx 2.6$ what gives $\beta_1 = 0.33$, $\beta_2 = 0.67$ and the constraint (3.1) is not fulfiled). However, inclusion of spins changes the angular dependence of the hard scattering; for spin 1/2 quarks the value of α appears to be essentially smaller and is of order 0.3 for almost all CIM amplitudes with 6 quarks. Now we have $\beta_1 = 0.1$, $\beta_2 = 0.9$ and the condition (3.1) is satisfied to a good approximation. Thus the CIM with spin 1/2 quarks is able to reproduce the weak rapidity dependence observed experimentally.

On the other hand, models without or with very soft angular dependence *at fixed s* have too fast fall-off in y and are excluded by our analysis: for $h(\lambda) = \text{const}$ we have $\alpha = 4$, $\beta_1 = 0.6$, $\beta_2 = 0.4$ and (3.1) is badly violated. It can be seen in Fig. 2, where $B(y)$ for $\alpha = 4$, $\langle x_{T1} \rangle = 0.2$ is plotted.

The authors are grateful to A. Białas and to R. Wit for continuous help during the course of this work, for useful remarks and for critical reading of the manuscript.

APPENDIX

In this Appendix we present the calculation leading to the formula (2.14). The first step is to perform the trivial integration over angles in (2.3). The result is

$$\left(\frac{\frac{d\sigma}{d^3p_1}}{E_1}\right)_{AB\to 1+X} = \int dx_{c_1} G_{c_1|A}(x_{c_1}) \int dx_{c_2} G_{c_2|B}(x_{c_2})$$

$$\times \int_{x_1}^{1} \frac{d\hat{x}_1}{\hat{x}_1^2} G_{1|J_1}(\hat{x}_1) \delta(\hat{s}+\hat{t}+\hat{u}) \left(\frac{d\sigma_H}{d\hat{t}}\right) + (A \leftrightarrow B). \tag{A.1}$$

Since the phase-space limits in (2.1) are

$$0 = \hat{s}+\hat{t}+\hat{u} = x_{c_1}x_{c_2}s + \frac{x_{c_1}}{\hat{x}_1} t_1 + \frac{x_{c_2}}{\hat{x}_1} u_1,$$

$$x_{c_1} < 1, \quad x_{c_2} < 1, \quad \frac{x_{c_1}}{\hat{x}_1} t_1 + \frac{x_{c_2}}{\hat{x}_1} u_1 < 0,$$

the symmetrization $A \leftrightarrow B$ (or $t_1 \leftrightarrow u_1$) of the integral is equivalent to the symmetrization ($x_{c_1} \leftrightarrow x_{c_2}$, $\hat{t} \leftrightarrow \hat{u}$) of the integrand.

Let us consider first the case when $G_{c_1|A}(x) = G_{c_2|B}(x) \equiv G_c(x) = \frac{n_c}{x}(1-x)^{q_c}$. Then the only part of the integrand in (2.1) which should be symmetrized is $f(\hat{t}/\hat{s})$ and to obtain the symmetrized expression one has only to replace $f(\hat{t}/\hat{s})$ by $f_{sym} = f(\hat{t}/\hat{s}) + f(\hat{u}/\hat{s}) = h(\lambda)$, where $\lambda = \frac{\hat{s}^2}{4\hat{t}\hat{u}} = \frac{1}{\sin^2\hat{\theta}_{J_1}} = \cosh^2\hat{y}_{J_1}$ (see (2.7)).

To perform the integrals in (5.1) it is convenient to change variables

$$x_{c_1}, x_{c_2} \to M, Y; x_{c_1} = \frac{M}{\sqrt{s}} e^{Y}, \quad x_{c_2} = \frac{M}{\sqrt{s}} e^{-Y}$$

where M, Y are mass and rapidity of c_1c_2 system. We have

$$\left(\frac{d\sigma}{\frac{d^3p_1}{E_1}}\right)_{AB\to 1+X} = \frac{2}{\pi}\frac{c_0}{(2p_{T1})^{2n}}\int_{x_1}^{1}\frac{d\hat{x}_1}{\hat{x}_1^2}\hat{x}_1^{2n}G_{1|J_1}(\hat{x}_1)$$

$$\times \int dY F_c\left(\frac{M}{\sqrt{s}}e^{Y}\right)F_c\left(\frac{M}{\sqrt{s}}e^{-Y}\right)H(\cosh^2(Y-y_1))$$

where $F_c(x) = xG_c(x)$, $M = 2p_{TJ_1}\cosh(Y-y_1)$, $H(\lambda) = \frac{1}{\lambda^n}h(\lambda)$.

To perform the integration over Y we note that the integrand is a product of two strongly peaked functions of Y, which for the integration purposes can be approximated by the Gaussian shapes

$$1.\quad F_c\left(\frac{M}{\sqrt{s}}e^{Y}\right)F_c\left(\frac{M}{\sqrt{s}}e^{-Y}\right) = n_c^2\left[\left(1-\frac{M}{\sqrt{s}}e^{Y}\right)\left(1-\frac{M}{\sqrt{s}}e^{-Y}\right)\right]^{g_c}$$

$$\approx n_c^2\left(\sqrt{(1-\tfrac{1}{2}x_{TJ_1}e^{y_1})(1-\tfrac{1}{2}x_{TJ_1}e^{-y_1})} - \tfrac{1}{2}x_{TJ_1}\right)^{2g_c}e^{-2g_c x_{TJ_1}\chi(x_{TJ_1},\,y_1)\,(Y-Y_0)^2}$$

$$\overset{*}{\approx} e^{-g_c(1+\cosh y_1)x_{TJ_1}}e^{-2g_c x_{TJ_1}(Y-Y_0)^2},$$

where

$$Y_0 = \tfrac{1}{2}(y_1+\bar{y}_1) \overset{*}{\approx} \tfrac{1}{2}y_1, \quad \bar{y}_1 = \tfrac{1}{2}\ln\frac{1-\frac{1}{2}x_{TJ_1}e^{y_1}}{1-\frac{1}{2}x_{TJ_1}e^{-y_1}} \overset{*}{\approx} 0,$$

$$\chi(x_{TJ_1}, y_1) = \frac{\sqrt{(1-\frac{1}{2}x_{TJ_1}e^{y_1})(1-\frac{1}{2}x_{TJ_1}e^{-y_1})}}{\left(\sqrt{(1-\frac{1}{2}x_{TJ_1}e^{y_1})(1-\frac{1}{2}x_{TJ_1}e^{-y_1})} - \frac{1}{2}x_{TJ_1}\right)^2} \overset{*}{\approx} 1$$

and the equalities with $*$, used in the following, are approximately satisfied for small x_1 and y_1; 2. $H(\lambda)$ decreases for large λ due to the factor $1/\lambda^n$ in almost all proposed hard scattering models. Thus we can approximate

$$H(\lambda) = H(\cosh^2\hat{y}_{J_1}) \approx H(1)e^{-\alpha(Y-y_1)^2}.$$

Within simplifications introduced above the integral over Y can be performed and the result for small x_1, y_1 reads

$$\left(\frac{d\sigma}{\frac{d^3p_1}{E_1}}\right)_{AB\to 1+X} = \int_{x_1}^{1} \frac{c_{J_1}}{p_{T1}^N}\,\hat{x}_1^{N-2} G_{1|J_1}(\hat{x}_1) e^{-b(x_{TJ_1},y_1)x_{TJ_1}} d\hat{x}_1,$$

where $N = 2n$ and

$$b(x_{TJ_1}, 0) = b(0,0) \equiv b_0 = 2g_c,$$

$$b(x_{TJ_1}, y_1) = b_0\left[\frac{\alpha}{b_0 x_{TJ_1}+\alpha}\cosh y_1 + \frac{b_0 x_{TJ_1}}{b_0 x_{TJ_1}+\alpha}\,\tfrac{1}{2}\,(1+\mathrm{ch}\, y_1)\right],$$

$$c_{J_1} = \frac{2}{\pi}\,\frac{c_0}{4^N}\, n_c^2 H(1)\sqrt{\frac{\pi}{b_0 x_{TJ_1}+\alpha}}\,.$$

To integrate over x_1 we note that since $G_{1|J_1}(x_1) = n_{1|J_1}\dfrac{1}{\hat{x}_1}(1-\hat{x}_1)^{g_{1|J_1}}$, the integrand contains the factor $\hat{x}_1^{N-2}(1-\hat{x}_1)^{g_{1|J_1}}$ and thus is strongly peaked for some $x_1 = \langle x_1\rangle$. From the mean value theorem we can write

$$\left(\frac{d\sigma}{\frac{d^3p_1}{E_1}}\right)_{AB\to 1+X} = \int_{x_1}^{1} d\hat{x}_1\,\frac{c_{J_1}}{p_{T1}^N}\,\hat{x}_1^{N-2} G_{1|J_1}(\hat{x}_1) e^{-b\left(\frac{x_{T1}}{\hat{x}_1},\, y_1\right)\frac{x_{T1}}{\hat{x}_1}}$$

$$\approx \frac{c_{J_1}}{p_{T1}^N}\, e^{-B(x_{T1},y_1)x_{T1}} \int_0^1 d\hat{x}_1 \hat{x}_1^{N-2} G_{1|J_1}(\hat{x}_1) \qquad \text{(A.2)}$$

where $B(x_1, y_1) = \dfrac{1}{\langle\hat{x}_1\rangle}\, b\left(\dfrac{x_{T1}}{\langle\hat{x}_1\rangle}, y_1\right)$. Denoting $B(x_1, 0) = B(0,0) = B$ we have

$$B(x_{T1}, y_1) = B\left[\frac{Bx_{T1}}{Bx_{T1}+\alpha}\,\tfrac{1}{2}\,(1+\cosh y_1) + \frac{\alpha}{Bx_{T1}+\alpha}\cosh y_1\right].$$

The last step is to calculate B. From (A.2) we find

$$B = \left(\frac{\dfrac{\partial}{\partial x_{T1}}\displaystyle\int d\hat{x}_1 \hat{x}_1^{N-2} G_{1|J_1}(\hat{x}_1) e^{-b_0\frac{x_{T1}}{\hat{x}_1}}}{\displaystyle\int d\hat{x}_1 \hat{x}_1^{N-2} G_{1|J_1}(\hat{x}_1) e^{-b_0\frac{x_{T1}}{\hat{x}_1}}}\right)_{x_{T1}=0} = b_0\left(1+\frac{g_{1|J_1}+1}{N-3}\right)$$

what menas that $\langle x_1\rangle = \dfrac{N-3}{N-2+g_{1|J_1}}$.

Up to now we have limited ourselves to the case when $G_{c_1|A}(x) = G_{c_2|B}(x)$. However, for small x_1, y_1 our results can be easily generalized to the non-symmetric case. Generally, after the symmetrization $A \leftrightarrow B$ we have under the integral

$$\left[G_{c_1|A}(x_{c_1})G_{c_2|B}(x_{c_2})f\left(\frac{\hat{t}}{\hat{s}}\right)\right]_{\text{sym}}$$

$$= G_{c_1|A}(x_{c_1})G_{c_2|B}(x_{c_2})f\left(\frac{\hat{t}}{\hat{s}}\right) + G_{c_1|A}(x_{c_2})G_{c_2|B}(x_{c_1})f\left(\frac{\hat{u}}{\hat{s}}\right)$$

$$= \frac{n_{c_1|A}n_{c_2|B}}{x_{c_1}x_{c_2}}\left[(1-x_{c_1})(1-x_{c_2})\right]^{\frac{1}{2}(g_{c_1|A}+g_{c_2|B})}\left[f\left(\frac{\hat{t}}{\hat{s}}\right)+f\left(\frac{\hat{u}}{\hat{s}}\right)\right]\tilde{\theta}, \tag{A.3}$$

where

$$\tilde{\theta} = \left(\frac{1-x_{c_1}}{1-x_{c_2}}\right)^{\frac{1}{2}(g_{c_1|A}-g_{c_2|B})} \frac{f\left(\frac{\hat{t}}{\hat{s}}\right)}{f\left(\frac{\hat{t}}{\hat{s}}\right)+f\left(\frac{\hat{u}}{\hat{s}}\right)} + (x_{c_1} \leftrightarrow x_{c_2}, \hat{t} \leftrightarrow \hat{u}).$$

Since $\hat{\theta}$ varies with Y much slower than the first, symmetric part of (5.3), we can proceed as before with the symmetric part, taking $g_c = \frac{1}{2}(g_{c_1|A}+g_{c_2|B})$ and finally use the mean value theorem in the integration over Y, taking $\hat{\theta}$ for $Y = \langle Y\rangle = \frac{Bx_{T1}Y_0+\alpha y_1}{Bx_{T_1}+\alpha}$. One can easily verify, that $\hat{\theta}(\langle Y\rangle) = 1$ for $y_1 = 0$ and for small x_1, y_1

$$\tilde{\theta}(\langle Y\rangle) \approx 1-(g_{c_1|A}-g_{c_2|B})x_{TJ_1}\sinh y_1 \frac{f\left(\frac{\hat{t}}{\hat{s}}\right)-f\left(\frac{\hat{u}}{\hat{s}}\right)}{f\left(\frac{\hat{t}}{\hat{s}}\right)+f\left(\frac{\hat{u}}{\hat{s}}\right)}$$

what gives a correction ΔB to the slope B. ΔB can be bounded for any $f(\hat{t}/\hat{s})$

$$\frac{|\Delta B|}{B} < \left|\frac{g_{c_1|A}-g_{c_2|B}}{g_{c_1|A}+g_{c_2|B}}\tanh y_1\right|$$

and can be simply neglected on this approximation level for most typical processes $\left(\text{e.g. } \frac{|\Delta B|}{B} < 0.16 \text{ for } Mq \to Mq \text{ in CIM at } y_1 = 0.75\right)$.

Thus our final result reads

$$\left(\frac{d\sigma}{\frac{d^3p_1}{E_1}}\right)_{AB\to 1+X} = \frac{c_{1|J_1}}{p_{T1}^N}e^{-B(x_{T1},y_1)x_{T1}} + (J_1 \leftrightarrow J_2)$$

where

$$B(x_{T1}, 0) = B(0, 0) \equiv B = \frac{1}{\langle \hat{x}_1 \rangle} (g_{c_1|A} + g_{c_2|B}),$$

$$\langle \hat{x}_1 \rangle = \frac{N-3}{N-2+g_{1|J_1}},$$

$$B(x_{T1}, y_1) = B\left[\frac{Bx_{T1}}{Bx_{T1}+\alpha} \tfrac{1}{2}(1+\cosh y_1) + \frac{\alpha}{Bx_{T1}+\alpha} \operatorname{ch} y_1\right],$$

$$c_{1|J_1} = \langle \hat{x}_1^{N-2} \rangle_{J_1} c_{J_1},$$

$$c_{J_1} = \frac{2}{\pi} \frac{c_0}{2^N} n_{c_1|A} n_{c_2|B} H(1) \sqrt{\frac{\pi}{Bx_{T1}+\alpha}},$$

$$\langle \hat{x}_1^{N-2} \rangle_{J_1} = \int_0^1 d\hat{x}_1 \hat{x}_1^{N-2} G_{1|J_1}(\hat{x}_1) = n_{1|J_1} \frac{(g_{1|J_1})!(N-3)!}{(N-2+g_{1|J_1})!}.$$

REFERENCES

[1] F. W. Büsser et al., *Phys. Lett.* **46B**, 471 (1973).

[2] K. Eggert et al., *Nucl. Phys.* **B98**, 73 (1975).

[3] P. Darriulat et al., *An Inclusive Measurement of Charged Particles Accompanying a High Transverse Momentum π^0 at the ISR Split Field Magnet Facility*, Contribution G5–21 to the International Conference on High-Energy Physics, Palermo (Italy) 23–28 June 1975.

[4] B. Alper et al., *Production Spectra of $\pi^{\pm}$, $K^{\pm}$, $p^{\pm}$ at Large Angles in Proton-Proton Collisions in the CERN–ISR*, CERN preprint, July 1975.

[5] R. Blankenbecler, S. J. Brodsky, J. Gunion, *Phys. Rev.* **D6**, 2652 (1973).

[6] S. J. Brodsky, G. R. Farrar, *Phys. Rev. Lett.* **31**, 1153 (1973); *Phys. Rev.* **D11**, 1309 (1975).